Localization-Delocalization Transition in a System of Quantum Kicked Rotors

C. E. Creffield, G. Hur, and T. S. Monteiro

Department of Physics and Astronomy, University College London, Gower Street, London WC1E 6BT, United Kingdom

(Received 6 May 2005; revised manuscript received 26 October 2005; published 19 January 2006)

The quantum dynamics of atoms subjected to pairs of closely spaced δ kicks from optical potentials are shown to be quite different from the well-known paradigm of quantum chaos, the single δ-kick system. We find the unitary matrix has a new oscillating band structure corresponding to a cellular structure of phase space and observe a spectral signature of a localization-delocalization transition from one cell to several. We find that the eigenstates have localization lengths which scale with a fractional power $L \sim \hbar^{-0.75}$ and obtain a regime of near-linear spectral variances which approximate the "critical statistics" relation $\Sigma_2(L) \simeq \chi L \approx \frac{1}{2}(1-\nu)L$, where $\nu \approx 0.75$ is related to the fractal classical phase-space structure. The origin of the $\nu \approx 0.75$ exponent is analyzed.

DOI: 10.1103/PhysRevLett.96.024103 PACS numbers: 05.45.Mt, 05.60.−k, 32.80.Pj, 72.15.Rn

The δ-kicked quantum rotor (QKR) is one of the most studied paradigms of quantum chaos. Its implementation using cold atoms in optical lattices [1] provided a convincing demonstration of a range of quantum chaos phenomena including dynamical localization [2], the quantum suppression of chaotic diffusion. Recently, an experimental study [3] of cesium atoms subjected to *pairs* of δ kicks (2δ-KR) showed surprisingly different behavior. The classical phase space is chaotic but is made up of fast-diffusing regions which are partly separated by slow-diffusing "trapping regions," where the classical trajectories stick; the classical analysis revealed a regime of anomalous diffusion corresponding to long-lived correlations between kicks.

Further details are given in Ref. [4], but we show here that the 2δ-KR has some unexpected *quantum* properties. We show that there is a cellular phase-space structure which arises from a novel oscillatory band structure of the corresponding unitary matrix. One consequence is a new type of localization-delocalization transition not seen in the QKR, where states delocalize from single- to multiple-cell occupancy; we show it has a clear spectral signature. We have also found scaling behavior of the localization lengths associated with a *fractional* exponent, i.e., $L \sim \hbar^{-0.75}$, whereas for the well-studied QKR, $L \sim \hbar^{-1}$. A similar exponent is found for the decay of return probabilities in the trapping regions, $P(t) \sim t^{-0.75}$. We argue that the exponent 0.75 corresponds closely to the value obtained for the dominant exponent of the golden ratio cantorus [5,6]. We show that the spectral fluctuations [both the nearest-neighbor statistics (NNS) and spectral variances] show important differences with the QKR in regimes where the delocalization of eigenstates is hindered by cantori bordering the cells. We find a regime approximating the form found in "critical statistics": The number variances of the spectra are linear $\Sigma_2(L) \simeq \chi L$ for $L \gg 1$, where $\chi \simeq 1/2(1-\nu) < 1$ and $\nu \simeq 0.75$.

The term critical statistics arose originally in relation to the metal insulator transition (MIT) in systems with disorder [7,8]. A new universal form of the distribution of nearest-neighbor eigenvalue spacings, termed "semi-Poisson," $P(s) \sim s\exp(-2s)$ was associated with the MIT [7]. For critical statistics, a very interesting connection has been established between the multifractal characteristics of the wave functions and those of the spectral fluctuations [8]: The number variances of the spectra are linear $\Sigma_2(L) \simeq \chi L$ for $L \gg 1$. The slope $\chi \simeq 1/2(1 - D_2/D) < 1$ was shown to be related to a fractal dimension D_2 obtained from the second moment of the wave function and to D, the spatial dimension of the system. For integrable dynamics, in contrast, $\Sigma_2(L) = L$, while for the Gaussian orthogonal ensemble (GOE), $\Sigma_2(L) \sim Ln(L)$. There is much current interest in so-called critical statistics in non–Kolmogorov-Arnold-Moser (KAM) billiards (typically systems where the dynamics would be integrable were it not for a discontinuity in the potential) [9], which show multifractal scalings and linear variances related to D_2. Below, we apply the term critical statistics in this broader sense, rather than the MIT critical point. Multifractal behavior has been demonstrated for Cantor spectra [10] where the level density itself is not smooth. However, until now, critical statistics have not been seen in—and were not thought to be relevant to—KAM systems. These are systems, ubiquitous in many areas of physics, where the transition to chaos as a perturbing parameter is increased is quite gradual.

The Hamiltonian of the 2δ-KR is $H(x, p) = (p^2/2) + K\cos x \sum_n \delta(t - nT) + \delta(t - nT + \epsilon)$; there is a short time interval ϵ between the kicks in each pair and a much longer time $\simeq T$ between the pairs themselves. In experiments, $\epsilon \sim 0.01$–$0.1 \ll T$ and $\hbar \simeq 2 - 1/4$ in the usual rescaled units [3].

A study of the spectral fluctuations of a time-periodic system involves a study of the eigenstates and eigenvalues of the one-period time-evolution operator $U(T, 0)$. For the QKR, the matrix representation, in an angular momentum basis $|l\rangle$, has elements $U_{lm} = U_l^{\text{free}} U_{lm}^{\text{kick}} = \exp(-il^2T\hbar/2)J_{l-m}(\frac{K}{\hbar})$. The "kick" terms $J_{l-m}(\frac{K}{\hbar})$ are Bessel functions and give the matrix the banded form

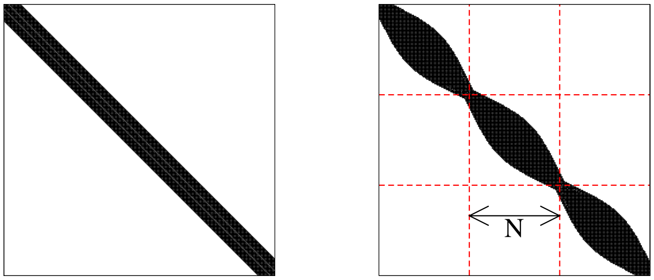

FIG. 1 (color online). Left: Structure of time-evolution matrix $U(T, 0)$, for the QKR, in a basis of momentum states, exemplifying the typical band structure of a band random matrix. Right: $U(T, 0)$ for our system, the 2δ-KR, showing the new form with oscillating bandwidth. Before delocalization, eigenstates are confined within a single "momentum cell" of dimension N.

illustrated in Fig. 1(a). Since $J_{l-m}(x) \simeq 0$ if $|l - m| > x$, we define the usual bandwidth $b = K/\hbar$. The resulting statistics are approximated by those of band random matrix theory (BRMT) [11] rather than of RMT: i.e., if the dimension of the $U(T, 0)$ matrix is $N_{\rm tot}$, the statistics are *Poissonian* for $N_{\rm tot} \gg b$; the eigenstates of the BRMT are exponentially localized in l, with a localization length in momentum ($p = l\hbar$) which equals $L_p \sim K^2/\hbar$, so states separated in p by $\gg L_p$ will be largely uncorrelated.

For the 2δ-KR, the corresponding matrix elements are

$$U_{lm} = e^{-il^2(T-\epsilon)\hbar/2} \sum_k J_{l-k}\left(\frac{K}{\hbar}\right) J_{k-m}\left(\frac{K}{\hbar}\right) e^{-ik^2/2\hbar\epsilon}. \quad (1)$$

As the $U(T, 0)$ matrix is quite insensitive to $(T - \epsilon)$, the quantum dynamics largely depends only on two scaled parameters $K_\epsilon = K\epsilon$ and $\hbar_\epsilon = \hbar\epsilon$, rather than on K, ϵ, and $\hbar$ independently: The remainder of the matrix is invariant if K_ϵ and $\hbar_\epsilon$ are kept constant.

An analytical form for the bandwidth of $U(T, 0)$ was obtained in Ref. [4]: The bandwidth oscillates sinusoidally between a maximum value $b_{\max} = 2K/\hbar$ for angular momenta $l \simeq 2n\pi/(\hbar\epsilon)$ and a minimum value $b_{\min} \approx 0$ for $l \simeq (2n + 1)\pi/(\hbar\epsilon)$. These minima correspond to the trapping momenta $p = l\hbar \simeq (2n + 1)\pi/\epsilon$ seen in experiment. The corresponding band structure of U is illustrated in Fig. 1(b): The band oscillates, and U is approximately partitioned into submatrices of dimension $N = \frac{2\pi}{\epsilon\hbar}$ corresponding to separate momentum cells.

The key to our work is our ability to vary the *transport* between the cells (by opening or closing the classical fractal "gates" between them) separately from the degree of *filling* of each individual cell. We begin by introducing a "filling factor" R, where

$$R = \frac{K^2}{N\hbar^2} = \frac{K_\epsilon^2}{2\pi\hbar_\epsilon} \quad (2)$$

measures the degree of filling of a cell by a typical state in the absence of confinement. Clearly, if there is no transport between cells, the states simply fill the cell uniformly, and, even if $R \gg 1$, the localization lengths $L_p \sim N\hbar$. We begin by defining a *localized* limit, where $R \ll 1$ and $L_p \ll N\hbar \sim \frac{2\pi}{\epsilon}$; typical states are insensitive to the boundary conditions of the cell, and this limit is Poissonian. At the other extreme, if we allow strong coupling between cells, we move to an opposite limit as an increasing proportion of eigenstates become delocalized over several cells.

We now investigate the transport. A classical analysis [4,12] shows that, if we take $K\epsilon \ll 1$ and expand initial momenta of the jth trajectory about the trapping values $p_j = (2n + 1)\pi/\epsilon + \delta p_j$, we can show that much of the trapping region is given by a classical map quite similar to the well-known standard map:

$$p_{j+2} \simeq p_j - K^2 \frac{\epsilon}{2} \sin(2x_j) - K\delta p^j \epsilon \cos x_j, \quad (3)$$

$$x_{j+2} \simeq x_j + p_{j+2}T. \quad (4)$$

Over much of the trapping region, the second term in Eq. (3) is dominant, for parameter regimes of interest. Then the kick impulse has a $\pi/2$ phase relative to the full map [the 2-kick map gives a pair of $V'(x) = -\sin x$ type impulses] and a momentum-dependent effective kick strength $K' = K\epsilon\delta p_j$. A detailed study of classical phase space [12] shows that at low K' the resonance structure is locally quite similar to the standard map. Hence, in the regime $K\epsilon\delta p_j \sim 1$, we expect the "golden ratio" cantori, which result from the last invariant manifold of a KAM system, to provide the strongest barrier to transport [13]. Though we want $K\epsilon$ to be small, if $K\epsilon < 0.1$, phase space becomes too regular. Hence, here we find that the regime of interest is within the interval $0.1 \le K_\epsilon \le 0.7$.

We investigated the corresponding quantum transport by evolving a set of wave packets $\Phi(p, t)$ in time [where $\Phi(p, t = 0) = \delta(p)$] for a range of K_ϵ and $\hbar_\epsilon$, until the momentum spreading is arrested by dynamical localization at $t \simeq t_H$. The resulting probability distributions $|\Phi(p, t \gg t_H)|^2 = N(p)$ have a characteristic "staircase" structure, shown in Fig. 2(a). At each step, there is a steep drop in probability:

$$N(p)_+ = e^{-2d} N(p)_- \quad (5)$$

[where $N(p)_\pm$ represent probabilities before $(-)$ and after $(+)$ the step] concentrated over the trapping region ($\sim 1/6$ of a cell in every case [4]). The staircase tracks an exponential envelope $N(p) \sim \exp(-2|p|/L_{\rm exp})$, where $L_{\rm exp} = \frac{\pi}{\epsilon d}$. We average over several steps, to obtain d as a function of K_ϵ and $\hbar_\epsilon$. In Fig. 2(b), we show that, quite accurately, $d \propto \hbar_\epsilon^{0.75}/f(K_\epsilon)$, where $f(K_\epsilon)$ is some function of the scaled kick strength K_ϵ. We estimate

$$d \approx \frac{3.5\hbar_\epsilon^{0.75}}{K_\epsilon^3}. \quad (6)$$

The parameter d [defined by Eq. (5)] quantifies the transport between the cells and complements the filling factor R. The inner steps of the staircase have been seen in the

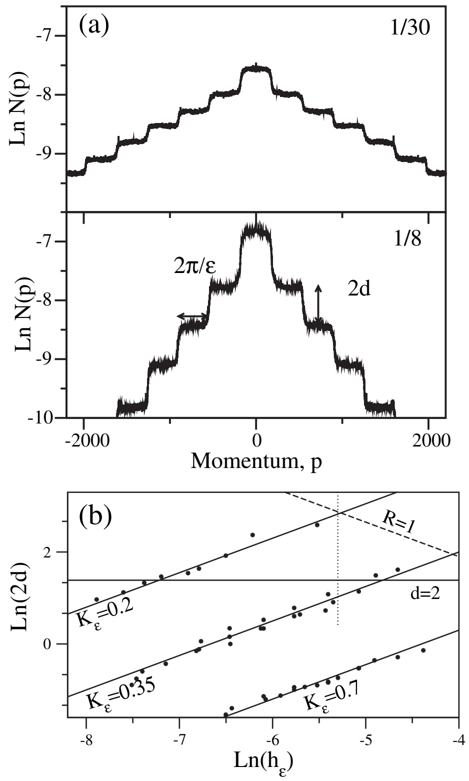

FIG. 2. (a) Final ($t \to \infty$) momentum distributions, $N(p)$ (slightly smoothed) for quantum wave packets of the 2δ-QKR for $K = 20$, $\epsilon = 0.0175$, and $\hbar = 1/8$ and $1/30$, respectively. $N(p)$ for both the eigenstates and wave packets shows a long-range staircase form, which on average follows the exponential $N(p) \sim \exp[-2(p - \bar{p})]/L_{\rm exp}$, where $L_{\rm exp}/2 = 2\pi/\hbar\epsilon$; the $\hbar$ dependence of $L_{\rm exp}$ is determined by the drop in probability d at each step. (b) $Ln(2d)$ plotted against $Ln(\hbar\epsilon)$ lies on straight lines of invariant $K_\epsilon = K\epsilon$, with constant slope 0.75. Hence, $d \propto (\hbar\epsilon)^{0.75}$ and $L_{\rm exp} \propto \hbar^{-0.75}$—in contrast with the well-known QKR result $L_{\rm exp} \propto \hbar^{-1}$. The $R = 1$ border is shown: For $R > 1$ (below the line), eigenstates fill much of a single cell. The *delocalization* border is shown at $d \simeq 2$: For $d > 2$ (above the line), over 98% of the probability of typical eigenstates is confined to a single cell; for $d < 2$, eigenstates begin to occupy multiple cells. Statistics are presented later in Fig. 3 for points corresponding to the dotted line.

momentum distributions of atoms in optical lattices [3,14]; therefore, though existing data are not in the critical regime, in principle, the form of d is experimentally verifiable.

We are unaware of another KAM system where a single power-law exponent is so dominant. Typically, power-law behavior is associated with mixed phase-space behavior, where many competing exponents are found [10]. We note also that the value 0.75 coincides closely with one of the scaling exponents found in Ref. [5] for the golden ratio cantori: These were $\sigma \approx 0.65$ (in the most unstable part of the cantori) and $\sigma \approx 0.76$ (most stable regions). There have been previous studies of transport in a region near golden ratio cantori. These have found $L \sim \hbar^{+0.66}$ [15] but only in a momentum band region ‘‘local’’ to the cantori. We note that the $L \sim \hbar^{+\sigma}$ dependence is associated with the physical process termed ‘‘retunneling’’ [6] associated with cantori which are classically ‘‘open’’ but for which $\hbar$ is too large to permit free quantum transport. An abrupt change to an $L \sim \hbar^{-\sigma}$ is observed when the cantori open for quantum transport and L is determined instead by localization. It has been argued that the reason all previous studies have found $L \sim \hbar^{+0.66}$ [6] is that the retunneling transport favors the unstable direction. To our knowledge, ours is the only example corresponding to the dominant exponent of the golden ratio cantori; we attribute this to the fact that we are always in a dynamical localization regime, and localization will select the most stable parts of the fractal cantori regions, where, at low K, elliptic fixed points are found.

We can now investigate the statistics as a function of the filling factor R and the intercell transport parameter d. Full details are given in Ref. [4], but in brief: We considered two types of boundary conditions (BCs). (1) Periodic BCs, i.e., solving the problem on a ‘‘torus’’ in momentum space, a well-known procedure for the QKR [11]. (2) Open BCs, where we diagonalize $U(T, 0)$ with $N_{\rm tot} = 10\,000$, but $N \approx 1000$; we then assigned the ith eigenstate to the nth cell if $(2n + 1)\pi/\epsilon \leq \langle p_i \rangle \leq (2n + 3)\pi/\epsilon$ and calculated statistics for each cell. In both cases, we averaged over ≈ 20 cells to improve significance. For periodic BCs, eigenstates cannot escape from a single cell of width $N\hbar$. For open BCs, however, they can delocalize onto neighboring cells.

In Fig. 3(a), the $\Sigma_2(L)$ statistics are presented. These represent the variances in the spectral number density $\Sigma_2(L) = \langle L^2 \rangle - \langle L \rangle^2$, where we consider a stretch of the spectrum with an average $\langle L \rangle$ levels. A fit to the best straight line in the range $L \simeq 5$–40 yields an estimate of the slope χ. In Fig. 3(b), we show the nearest-neighbor $P(S)$ statistics. We quantify the deviation of $P(S)$ from $P_P(S)$ and $P_{\rm GOE}(S)$, its Poisson and GOE limits, respectively, with a parameter Q [16]:

$$1 - Q = \frac{\int_0^{S_0}(P(S') - P_{\rm GOE}(S')dS')}{\int_0^{S_0}(P_P(S') - P_{\rm GOE}(S'))dS'}. \qquad (7)$$

Hence, $Q = 0$ indicates a Poisson distribution, while $Q = 1$ signals a GOE distribution. We take $S_0 = 0.3$.

The results of Fig. 3 demonstrate that the statistics are not too sensitive to boundary conditions for $d > 2$ (see also [4]). However, for $d \leq 2$, while the states with periodic BCs (effectively restricted to a matrix of dimension N) move gradually to the GOE limit, for the open BCs, at delocalization the statistics tend back to the Poisson limit. This initially surprising behavior occurs because, after delocalization, one finds increasing numbers of states for which $\langle p_i \rangle$ assigns them to the nth cell but for which much of the state's probability is actually found in neighboring cells [4]. Hence, states within each spectrum of N eigenvalues become progressively uncorrelated. This apparent

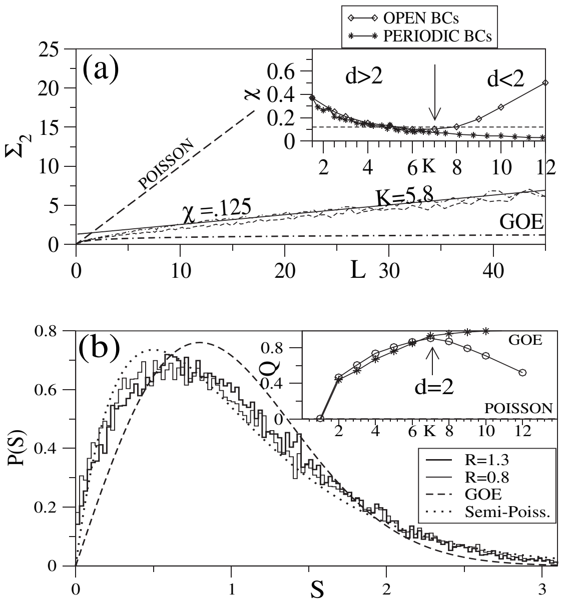

FIG. 3. (a) The $\Sigma_2(L)$ statistics for the 2δ-KR. Approximately linear variances with slope $\chi \approx 0.125$ are found in the intermediate regime. The solid line indicates the line $\Sigma_2(L) = 0.125L + c$ corresponding to the critical statistics slope $\chi \approx 1/2(1-\nu)$, where $\nu \simeq 0.75$ is the fractional exponent obtained previously. (b) Corresponding nearest-neighbor statistics for $R = 0.8$ and $R = 1.3$ of an intermediate form, which is compared with the semi-Poisson and GOE forms. The insets show the effect of the boundary conditions. Before delocalization ($d > 2$), the results are insensitive to boundary conditions. If $d < 2$, for periodic BCs (points indicated by asterisks), the statistics make a transition to GOE; for open BCs (points indicated by circles), the statistics tend to Poissonian behavior. The arrows indicate the $d = 2$ border.

failure of the procedure of assigning states to a given cell, in fact, provides a rather good "marker" for the onset of delocalization and yields a clear "turning point" in both the NNS and $\Sigma_2(L)$ behavior. A detailed study of the multicell regime remains to be undertaken; models of the statistics for chaotic systems with a nonuniform rate of exploration of phase space [17] may be relevant here.

Of further interest here is an intermediate regime, found for both boundary conditions for $R \approx 1$ and $d > 2$. Over a wide range of parameters and different cell sizes [4], we find approximately linear variances, for $L \gg 1$ and $L \ll N$, with slope $\chi \approx 0.125$. The inset in Fig. 3(a) plots the values of χ calculated along the vertical dotted line in Fig. 2(b) for periodic and open boundary conditions. We note that a study of the decay of return probabilities obtained $P(t) = |\langle\psi(t=0)|\psi(t)\rangle|^2 \sim t^{-0.75}$ for wave packets started in the trapping regions (see [4]). The value of $\chi \approx 0.125$ corresponds to the value which would be obtained from the MIT relation, $\chi \approx 1/2(1-D_2)$, if $D_2 \approx 0.75$; in the MIT, return probabilities with $P(t) \sim t^{-D_2}$ were similarly found. We suggest that this represents a KAM analogue of behavior associated with critical statistics.

In summary, we have shown that the behavior of the 2δ-kicked system is rather different from the standard QKR. We have identified a spectral signature of the novel localization-delocalization transition that the system exhibits. We have also identified signatures of the fractal phase-space structure of the cell borders. The trapping regions may have applications in atom optics experiments, as a means of manipulating the momentum distribution of the atomic cloud.

This work was supported by the EPSRC. We thank Shmuel Fishman and Antonio Garcia-Garcia for helpful comments and advice.

[1] F. L. Moore, J. C. Robinson, C. F. Bharucha, B. Sundaram, and M. G. Raizen, Phys. Rev. Lett. **75**, 4598 (1995).
[2] G. Casati, B. V. Chirikov, F. M. Izraelev, and J. Ford, in *Lecture Notes in Physics* (Springer, Berlin, 1979), Vol. 93, p. 334; S. Fishman, D. R. Grempel, and R. E. Prange, Phys. Rev. Lett. **49**, 509 (1982).
[3] P. H. Jones, M. M. Stocklin, G. Hur, and T. S. Monteiro, Phys. Rev. Lett. **93**, 223002 (2004).
[4] C. E. Creffield, S. Fishman, and T. S. Monteiro, physics/0510161.
[5] S. Fishman, D. R. Grempel, and R. E. Prange, Phys. Rev. A **36**, 289 (1987).
[6] N. T. Maitra and E. J. Heller, Phys. Rev. E **61**, 3620 (2000).
[7] B. I. Shklovskii *et al.*, Phys. Rev. B **47**, 11 487 (1993).
[8] J. T. Chalker, I. V. Lerner, and R. A. Smith, Phys. Rev. Lett. **77**, 554 (1996); V. E. Kravtsov and K. A. Muttalib, Phys. Rev. Lett. **79**, 1913 (1997); D. Braun, G. Montambaux, and M. Pascaud, Phys. Rev. Lett. **81**, 1062 (1998); F. Evers and A. D. Mirlin, Phys. Rev. Lett. **84**, 3690 (2000).
[9] E. B. Bogomolny, U. Gerland, and C. Schmit, Phys. Rev. E **59**, R1315 (1999); A. M. Garcia-Garcia and J. J. M. Verbaarschot, Phys. Rev. E **67**, 046104 (2003); E. Bogomolny and C. Schmit, Phys. Rev. Lett. **92**, 244102 (2004); A. M. Garcia-Garcia and J. Wang, Phys. Rev. Lett. **94**, 244102 (2005).
[10] R. Ketzmerick, G. Petschel, and T. Geisel, Phys. Rev. Lett. **69**, 695 (1992).
[11] M. Feingold *et al.*, Phys. Rev. B **31**, R6852 (1985); F. M. Izraelev, Phys. Rep. **196**, 299 (1990).
[12] M. Stocklin, Ph.D. thesis, University College London (to be published).
[13] E. Ott, *Chaos in Dynamical Systems* (Cambridge University Press, Cambridge, England, 1993).
[14] K. Vant, G. Ball, H. Ammann, and N. Christensen, Phys. Rev. E **59**, 2846 (1999).
[15] T. Geisel, G. Radons, and J. Rubner, Phys. Rev. Lett. **57**, 2883 (1986).
[16] C. Mejia-Monasterio, G. Benenti, G. G. Carlo, and G. Casati, Phys. Rev. A **71**, 062324 (2005).
[17] O. Bohigas, S. Tomsovic, and D. Ullmo, Phys. Rep. **223**, 43 (1993).